Frequency-dependent electrical characterization of rock types from Ewekoro, Eastern Dahomey Basin, Nigeria

O. B. Olatinsu[1], D. O. Olorode[1], M. Josh[2], B. Clennell[2] and L. Esteban[2]

[1]Department of Physics, Faculty of Science, University of Lagos, Lagos, Nigeria
[2]CSIRO Earth Science and Resource Engineering, 26 Dick Perry Ave, Kensington, Western Australia 6151

Dielectric measurements (40 Hz–110 MHz) conducted on samples of limestone and its associated rocks from Ewekoro, Eastern Dahomey Basin, Nigeria has yielded vital information for characterization. Cole–Cole plots manifest a distribution of relaxation times in the rock samples common for multicomponent systems. All the rock types show dielectric dispersion in dry and partially saturated conditions, but the frequency range differs for the rock types and depends on wettability. At partial water saturation there is: (i) enhanced polarization resulting in increase in real and imaginary permittivities; (ii) shortened region of dielectric dispersion; (iii) broadened electrode polarization plateau; and (iv) steeper and shorter dispersion region. Irrespective of the state of the rocks, dielectric parameters for shale and glauconite are at least an order greater than for limestone and sandstone. Geometric or textural effects are partly responsible for the observed differences coupled with the presence of charged clay/clay-like particles in shale and glauconite. Decrease in relaxation and critical frequencies in partial saturation for shale in contrast to the increase in these frequencies for the other three rock types is due the effect of pore geometry on overall dielectric relaxation. This study shows that dielectric measurement can complement geochemical analysis in laboratory evaluation and characterization of rock raw materials.

Keywords: Dielectric dispersion, frequency response, loss tangent, partial saturation, rock types.

THE identification and characterization of mineral deposits is important in the development and operation of mining and mineral processing for industrial purposes[1]. Laboratory analysis is an integral part of the quality assurance process, right from the testing of raw materials to the finished product[2]. Such analysis usually involves the determination of a wide range of associated properties and must be carried out based on the requirements of consuming industries[3]. Established procedures include geochemical, mineralogical, petrographic as well as geological evaluations. Frequency-dependent electrical measurements are a useful non-destructive method for characterizing porous rocks and soils. Also, the conductivity of a porous rock is related to microstructural properties such as porosity, poregeometry and surface morphology of the mineral grains lining the pores, as well as the dielectric properties of the mineral grains and pore fluid. It is therefore possible that the integration of dielectric analysis in large-scale evaluation of geologic formations can improve characterization of essential industrial rock minerals for economic usefulness.

Globally, limestone and its associated rocks such as shale and sandstone are the major raw materials for cement production[4]. Many limestone deposits, provided they are low in magnesia (MgO), easily meet the necessary requirements and a number of other lime-containing raw materials are known to be used. The lithofacies exposed at Ewekoro Eastern Dahomey Basin, Nigeria, include calcareous limestone and shale (Ewekoro Formation) overlain by dark grey to light grey shales (Oshosun Formation), and sandstones of the Ilaro Formation[5]. Glauconite bands, usually of low thickness, also occur along with other rocks at Ewekoro and various places of similar geological setting such as Sagamu, Ibese and Ilaro, all in southwest Nigeria[6]. This definite mineral (iron potassium phyllosilicate of mica group) of characteristic green colour with very low weathering resistance and friable, is usually a component of sedimentary rocks like sandstones and limestone in marine environments[7]. One problem usually associated with glauconite from several parts of the world is the high magnesia content, which makes it unsuitable for cement production. The other contentious issue with glauconite is that it is difficult to burn, which means more energy consumption. The homogeneity of feed chemical composition has an important relationship with fuel consumption, kiln operation, clinker formation and cement performance[8]. Hence this suggests the need for clear differentiation of glauconite from the other required rock raw materials.

Several electrical/dielectric tools have been employed in the investigation of rock properties[9,10]. The efficient use of these tools depends on the understanding of the mechanisms of dielectric behaviour of rocks[11–19]. Broadband

*For correspondence. (e-mail: oolatinsu@unilag.edu.ng)

frequency dielectric measurement of heterogeneous media is based on the strong relationship between the fluid content and dielectric permittivity. The electrical responses differ for dry and fluid-saturated rocks[20–22]. As a result of their sensitivity to ionic content and surface texture, dielectric measurements of saturated rocks exhibit frequency dispersions of dielectric properties[23,24]. In addition, surface contributions due to solid–liquid interface and clustering effects have to be taken into consideration for the determination of electrical properties[25–27].

Frequency-dependent properties of materials result from different mechanisms of charge transport and charge storage. Some of these mechanisms operate rapidly and are observed at relatively high frequencies, while slow mechanisms are observed at lower frequencies. At low frequencies, the electrical properties of rocks and minerals are dominated by charge transport or conduction mechanisms, whereas at high frequencies charge storage or polarization mechanisms dominate.

In geologic materials, dielectric dispersion is usually due to polarization in bulk sample. This is associated with charge build-up at grain boundaries or at grain imperfections in sample constituents (components) with different dielectric properties[28]. Materials with clay/clay-like constituents, for e.g. shale which are usually charged provide additional contribution to dielectric properties in rocks. For saturated rocks, due to their sensitivity to ionic content in addition to surface texture, dielectric measurements exhibit frequency dispersions of dielectric constant and electrical conductivity that are influenced by a variety of factors such as fluid saturation, porosity, pore morphology, etc. Knight and Abad[29] have shown that the dielectric constant of partially saturated sandstone varies as a function of the level of water saturation. Their experimental data indicate that rock–water interaction, at low saturation has a large effect on the measured dielectric response. Specific reference works are those by Fechner *et al.*[30] and Bekhit and Khalil[31] on limestone; Knight[12], Gomaa[22], Hu and Liu[32], and Szerbiak *et al.*[33] on sandstone; Josh *et al.*[10], Adisoemarta[17], Josh[19], Fam and Dusseault[34] and Sweeney *et al.*[35] on shale. This study focuses on the dielectric characterization of limestone, shale, sandstone and glauconite, which are the common lithologies at Ewekoro. The aim is to utilize the dielectric characteristics of these rocks as diagnostic tools for lithotype discrimination and characterization.

Materials and methods

Sample description and preparation

Twenty-two (22) rock samples (limestone – LM (8), sandstone – SA (4), shale – SH (5) and glauconite – GL (5)) were collected from the Ewekoro quarry site of Lafarge WAPCO cement factory. Specifically the sampling points fall within elevation 72–125 ft; lat. 6°54′–6°56′N; and long. 3°10′–3°12′E. The appearance and texture of the samples vary considerably even within each rock type. Table 1 summarizes the physical and textural descriptions of the samples. Preliminary sample preparation involved cutting the samples into approximately disc shape with the aid of a diamond saw. A range of sizes in diameter and thicknesses was obtained, depending on the size of the original lump of sample. The disk-shaped sample surfaces were later ground and polished using a surface grinder to obtain smooth, parallel faces. Due to porosity/pore spaces, sandstone samples generally retain a small degree of roughness. They were then kept in polyethylene bags and later in glass containers to avoid moisture absorption.

Geochemical analysis

Quantitative determination of elements and oxides in rock samples is an important task in geological, mineralogical and industrial evaluation[36]. Furthermore, determination of the elemental composition of the major industrial raw materials is an essential step in the characterization for industrial process[37]. Rock pieces obtained in the process of sample preparation were dried for several days and analysed for major and trace elements with the aid of atomic absorption spectrophotometer (AAS). Quantitative data on percentage chemical composition of elemental oxides such as SiO_2, Al_2O_3, Fe_2O_3, CaO, P_2O_5, TiO_2, K_2O, MnO, MgO and Na_2O were obtained using AAS.

Dielectric measurement

Dielectric measurements were carried out on dry and saturated samples of limestone, sandstone, shale and glauconitec of Ewekoro. The frequency range of the applied field was from 40 Hz to 110 MHz. The dielectric measuring system consisted of a precision impedance analyser (Agilent 4294A, Agilent Technologies Japan, Ltd) and parallel-plate dielectric cell developed by the Commonwealth Scientific and Industrial Research Organization Earth Science and Resource Engineering Unit of the Australian Resources Research Center, Kensington, Western Australia[10]. The output parameters from the analyzer are the parallel capacitance C_p and the parallel resistance R_P, from which both the real part of the relative dielectric permittivity (dielectric constant) ε'_r and the imaginary relative permittivity (dielectric loss) ε''_r as well the conductivity σ were calculated for each frequency using eqs (1)–(3) respectively. Also, the loss tangent D was computed from the ratio of ε''_r and ε'_r (eq. 4). Good electromagnetic shielding and electrode coupling were implemented to the whole-sample holder in order to minimize laboratory electromagnetic (EM) noise such as switching noise from power supplies. The material was mounted in a sample cell between the parallel circular electrodes, thus forming a sample capacitor.

Table 1. Physical and textural description of rock samples from Ewekoro, Eastern Dahoney Basin, Nigeria

Rock type	Colour	Texture
Limestone	Chalk white/light grey/grey/greenish-brown	Fine-to-medium/coarse grains
Sandstone	Brown/reddish-brown	Medium/coarse grains
Shale	Light grey/grey	Slate-like/laminated, smooth pelletal grains
Glauconite	Greenish	Hard, pelletal grains

$$\varepsilon_r'(\omega) = \frac{C_P(\omega)d}{\varepsilon_0 A}, \quad (1)$$

$$\sigma(\omega) = \frac{d}{R_P(\omega)A}, \quad (2)$$

$$\varepsilon_r''(\omega) = \frac{\sigma(\omega)}{\omega\varepsilon_0} = \frac{R_P^{-1}(\omega)d}{\omega\varepsilon_0 A}, \quad (3)$$

$$D = \frac{\varepsilon_r''}{\varepsilon_r'}, \quad (4)$$

where d is the distance between the electrodes, A their area, ω the radian frequency ($\omega = 2\pi f$) and ε_0 is the permittivity of free space. The diameter and thickness of the samples were measured using an electronic digital caliper. Measurement on shale samples in full saturation was not possible because they did not survive saturation. In the process they crumbled into laminated pieces due to their oily nature.

Results

Elemental oxides composition

Table 2 gives the major and trace element compositions of the analysed rock samples. Comparison of the average composition of these elements shows that there are some geochemical similarities between limestone and glauconite samples on one hand, as well as between sandstone and shale on the other. Proportion of lime (CaO) in limestone and glauconite is quite similar (above 90%). However, silica (SiO_2) content, although very low in both samples, is higher in some limestone than glauconite samples, while the trace elements composition is generally low and similar in the two rock types. In sandstone and shale samples, silica (above 55%), alumina (above 25%) and ferrous oxide (above 4.5%) are in similar proportions. Generally, magnesia (MgO) in limestone and glauconite is lower than in sandstone and shale. Hence from the geochemical data, it is evident that geochemical analysis alone may not be sufficient to discriminate the rock material deposits present at Ewekoro.

Cole–Cole plots

With the aid of the Cole–Cole plot[38], insights into the polarization and conduction mechanisms in the rocks were revealed. The Debye response has been frequently used to describe dielectric dispersion in a system with a single relaxation time[39,40]. For a Debye-type relaxation process in which a single relaxation time τ is assumed, this should produce a semi-circle with centre on the horizontal axis[25]. However, many materials, including rocks, deviate from Debye behaviour, suggesting the presence of a distribution of relaxation times. The plots for the rocks in this study are shown in Figure 1 (for dry rock samples) and Figure 2 (for partially saturated rock samples). Knight[11] as well as Knight and Nur[13] have established the existence of a critical frequency f_0 that separates the low frequency electrode polarization effects from high frequency bulk material polarization region of ε_r' for Berea sandstones. In the present study, only few samples depict this critical frequency. It is an indication that this frequency for these rocks is probably below 40 Hz, which is the lowest frequency covered in the study.

Dielectric dispersion

The physical mechanisms that influence the dielectric properties of matter are strongly dependent on the frequency of the electromagnetic field. Consequently, the real relative permittivity is also dependent on frequency (i.e. dispersive). Figure 3 (rocks in dry condition) and Figure 4 (rocks in partial saturation) show the variation of ε_r' with frequency for the rock samples. At frequencies away from relaxation frequency, a power-law dependence on frequency of ε_r' is a common manifestation in rocks and has been observed for sandstone[11,13]. This is commonly defined as the 'universal dielectric response'[41] and has been found to be due to the microgeometry of a material. This is also depicted by the rock samples in the present study, but the frequency range differs with rock types. These plots for dry and saturated samples show mainly an upper plateau of electrode polarization with nearly constant ε_r' and dispersion regions of decreasing ε_r' with frequency. The more saturated the samples, the wider the electrode polarization plateau. Also, the dispersion region becomes steeper and shorter with saturation. It can be seen that electrode polarization effect is more pronounced in shale and glauconite in dry condition. With the wet sample, the frequency separating the regions of electrode polarization effect and bulk material polarization shifts significantly to higher value by at least an order.

Table 2. Summary of geochemical analysis

Rock type	Sample	Proportion of elemental oxides (%)									
		SiO_2	Al_2O_3	Fe_2O_3	TiO_2	CaO	P_2O_5	K_2O	MnO	MgO	Na_2O
Limestone	LM1	3.76	1.07	0.12	–	53.35**	–	0.18	0.01	0.28	0.16
	LM2	2.69	0.56	0.24	–	54.64**	–	0.12	0.01	1.20	0.14
	LM3	2.66	0.46	0.16	–	54.86**	–	0.12	0.01	0.24	0.16
	LM4	0.79	0.60	0.40	–	55.97**	–	0.14	–	0.32	0.16
	LM5	3.64	0.82	1.90	–	55.21**	–	0.18	–	0.36	0.18
	LM6	0.72	0.56	0.40	–	54.64**	–	0.16	–	0.44	0.16
	LM7	0.84	0.60	0.16	–	54.92**	–	0.18	–	0.24	0.21
	LM8	0.71	0.26	0.16	–	54.86**	–	0.14	0.01	0.32	0.18
Glauconite	GL1	0.78	0.56	0.12	–	54.97**	–	0.09	–	0.18	0.16
	GL2	0.74	0.82	0.24	–	54.58**	–	0.16	0.02	0.34	0.22
	GL3	0.46	0.22	0.12	–	55.21**	–	0.12	–	0.08	0.18
	GL4	0.36	0.04	0.40	–	55.23**	–	0.12	0.01	0.18	0.18
	GL5	0.45	0.25	0.15	–	55.20**	–	0.12	0.01	0.11	0.21
Sandstone	SA1	57.95	28.06*	4.74#	1.12+	1.51	0.03	0.80	0.06	4.13	0.79
	SA2	58.54	26.06*	4.72#	1.17+	1.54	0.02	0.91	0.07	4.40	0.91
	SA3	59.38	27.06*	4.11#	1.15+	1.58	0.02	0.93	0.06	4.83	0.85
	SA4	58.53	27.93*	4.27#	1.10+	1.54	0.03	0.93	0.06	4.68	0.90
Shale	SH1	56.08	29.97*	4.81#	1.16+	1.59	0.01	0.87	0.08	4.56	0.83
	SH2	54.82	31.27*	4.98#	1.23+	1.61	0.01	0.85	0.08	4.29	0.83
	SH3	53.61	30.82*	5.30#	1.34+	1.74	0.01	1.14	0.08	4.93	0.92
	SH4	52.78	31.95*	5.25#	1.21+	1.70	0.01	0.89	0.07	5.21	0.90
	SH5	56.39	29.60*	4.66#	1.13+	1.66	0.01	0.89	0.07	4.69	0.87

Note rock types with similar elemental oxide composition are indicated with symbols *Al_2O_3; #Fe_2O_3; **CaO, +TiO_2. LM, Limestone; SA, Sandstone; SH, Shale; GL, Glauconite.

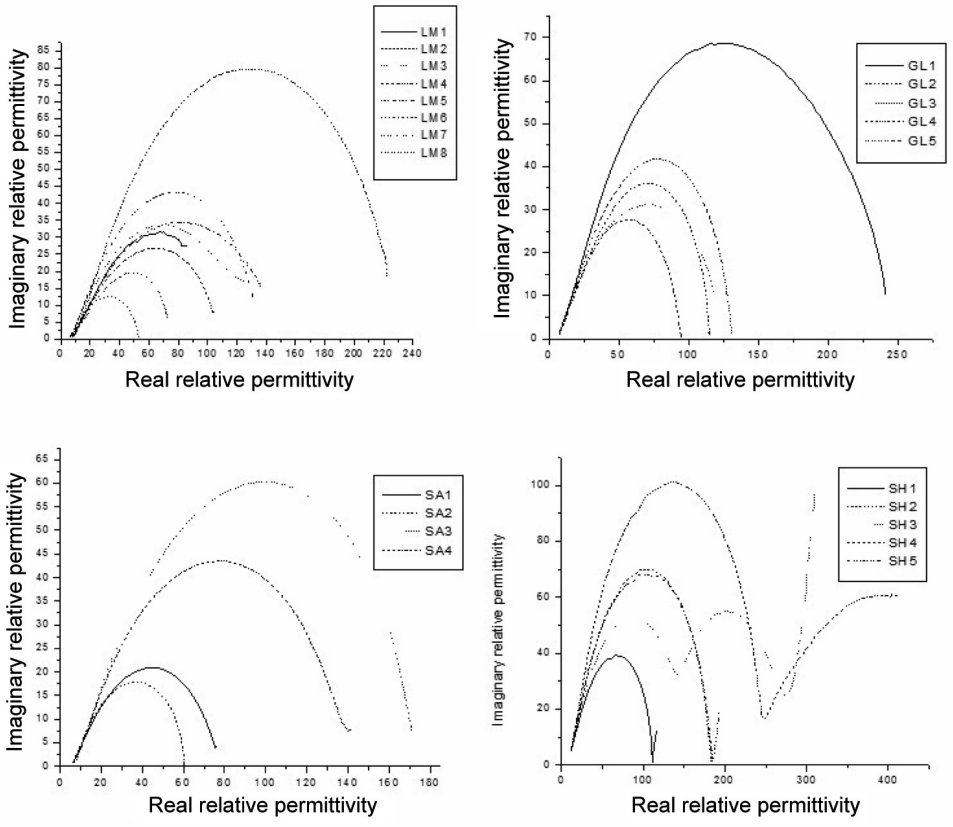

Figure 1. Cole–Cole plots for the dry rock exhibiting semicircular curve characteristic of dielectric relaxation. LM, Limestone; GL, Glauconite; SA, Sandstone and SH, Shale.

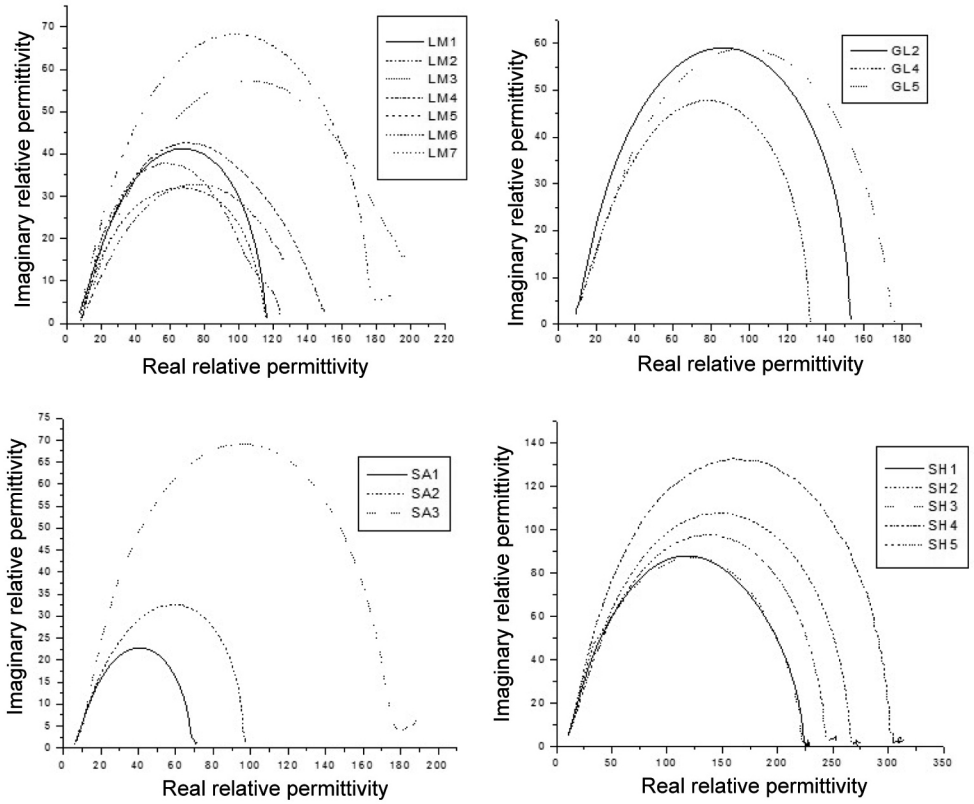

Figure 2. Cole–Cole plots for partially saturated samples. The more wet the samples become, the stronger the tail (low frequency segment).

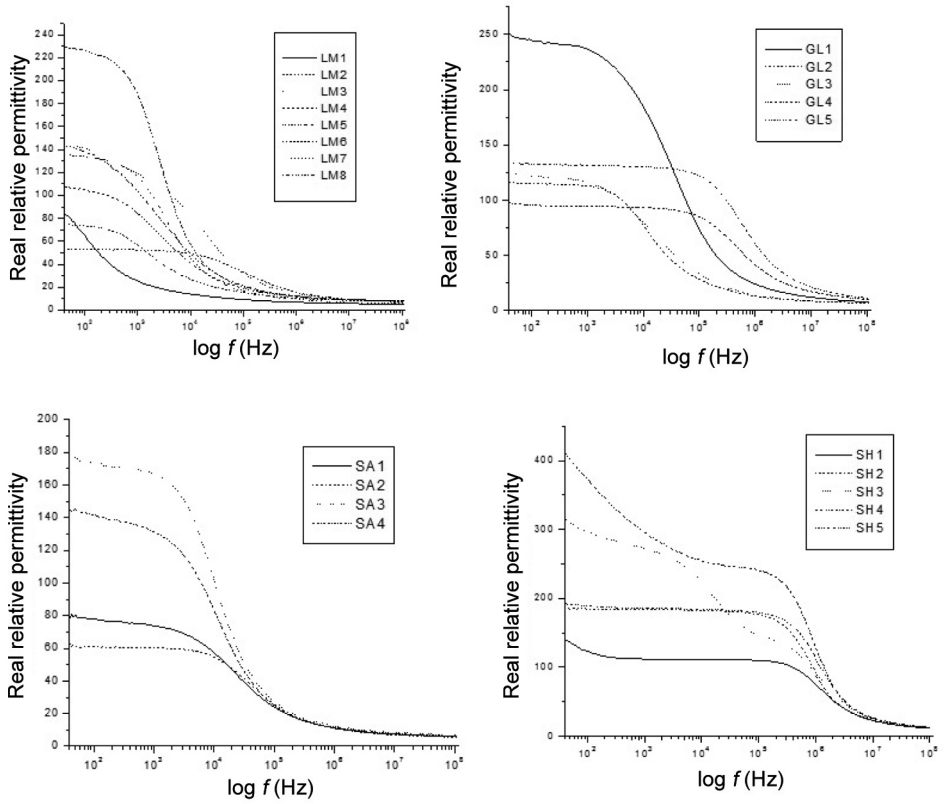

Figure 3. Plots of real relative permittivity versus frequency for dry samples showing end of plateau region at 10 kHz for sandstone, between 1 and 100 kHz for glauconite, 1 and 10 kHz for limestone and 1 MHz for shale.

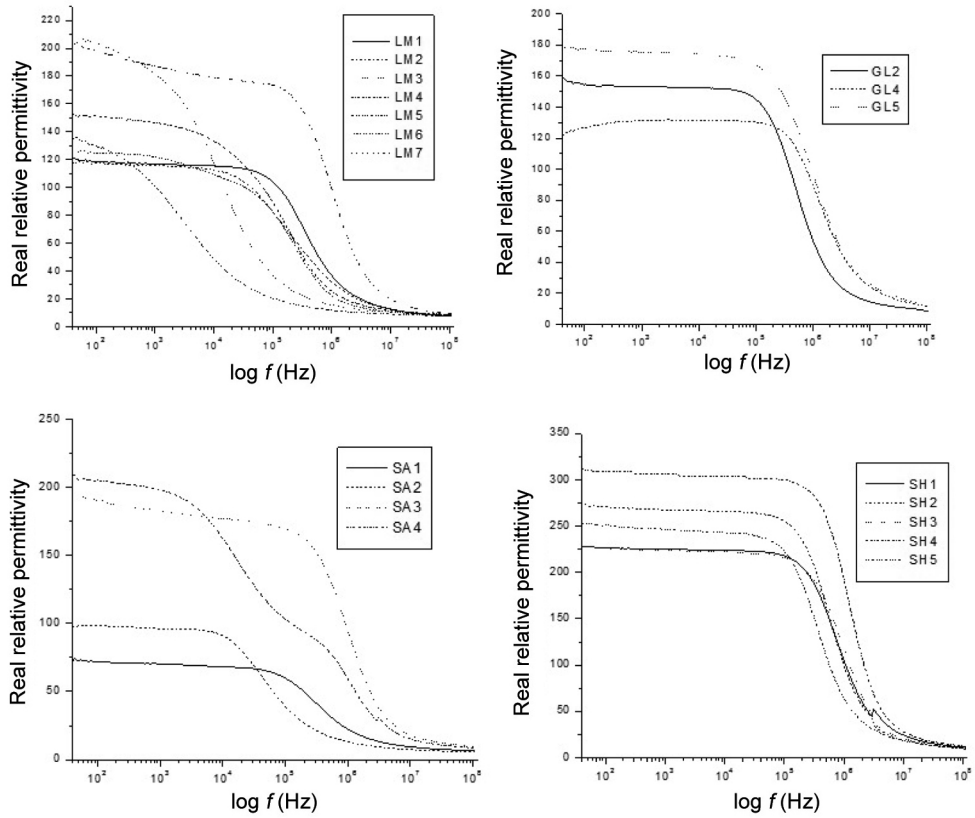

Figure 4. Plots of real relative permittivity versus frequency for partially saturated samples. Plateaus region ends at 10 kHz to 100 kHz for sandstone, 100 kHz–1 MHz for glauconite, 10 kHz to less than 100 kHz for limestone, and less than 1 MHz for shale.

Dielectric loss

The imaginary relative permittivity, ε_r'' directly relates to loss in a rock system due to polarization mechanisms. Under alternating current conditions, energy losses are significant because thermal agitation tries to randomize charge/dipole orientations. Hence there is lag in particles/dipole response to changing applied alternating field. The absorption of electrical energy by a dielectric material that is subjected to an alternating electric field is termed dielectric loss. Figure 5 (dry rocks) and Figure 6 (partially saturated rocks) show the behaviour of ε_r'' with frequency for the rock samples. Maximum absorption peaks with corresponding relaxation frequency are observed with dry and saturated samples, which show that the dominant mechanism is polarization. Significant shift in relaxation frequency to higher value is observed for limestone, glauconite and sandstone in wet condition, while for wet shale samples, there is a decrease in relaxation frequency.

Loss tangent

Loss tangent shows how much energy supplied by an external electric field is dissipated as motion and heat. It is the ratio of the loss component to the storage component or in-phase component to the quadrature component. This was calculated for both the dry and saturated rocks. The variation with frequency is shown in Figure 7 (dry rocks) and Figure 8 (partially saturated rocks). In imaginary relative permittivity curves (Figures 5 and 6), only the relaxation due to high frequency response is shown, with no information on low frequency or total response. The peak in loss tangent (D) is indicative of the total electrical response. The slope of loss tangent versus log frequency is proportional to the breadth of the time constant distribution[42]. The slope is equal to $1 - \alpha$ for $\omega\tau < 1$, and $-(1 - \alpha)$ for $\omega\tau > 1$. These plots show that at high frequencies, polarization is the dominant mechanism for the samples in dry and partial water saturation conditions. The double peak observed in shale sample SH3 is likely due to microfractures in the rock, possibly caused by two separate well-distinguished and non-communicating constituents.

Discussion

In dry conditions, both real and imaginary dielectric permittivity plots show frequency dispersion within certain frequency ranges. All the rock types show a plateau of nearly constant real relative permittivity, but with ranges

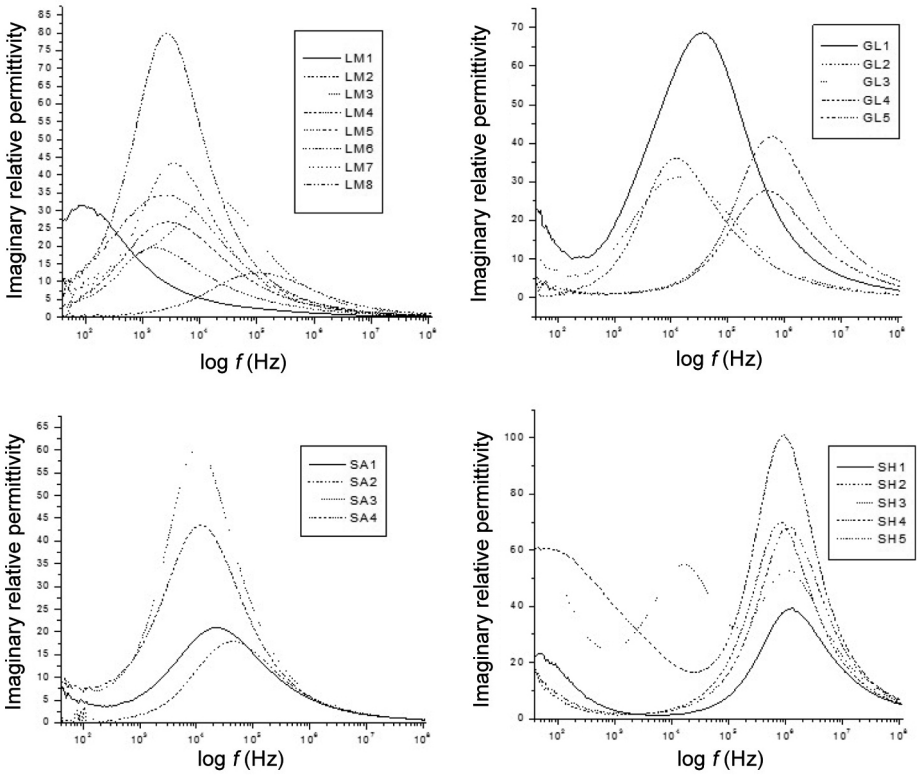

Figure 5. Plots of imaginary relative permittivity versus frequency for dry samples showing characteristic Debye response with sharp relaxation peaks occurring for most of the samples.

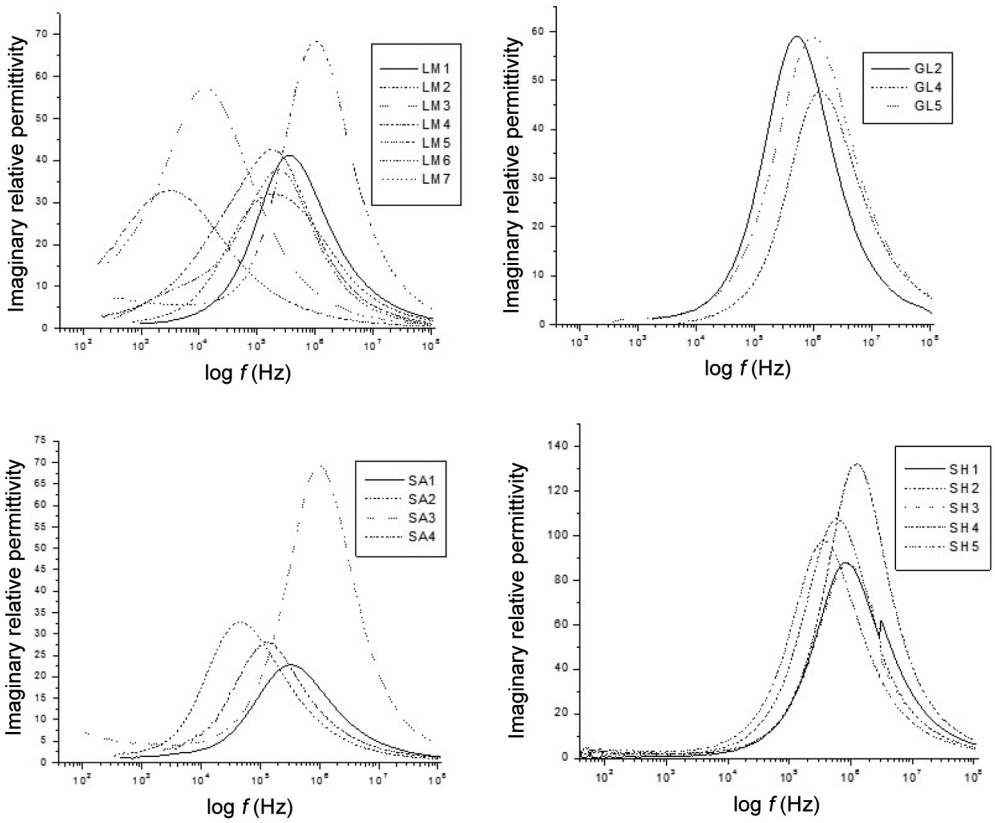

Figure 6. Plots of imaginary relative permittivity versus frequency for partially saturated samples. Relaxation peaks are shifted into higher frequencies.

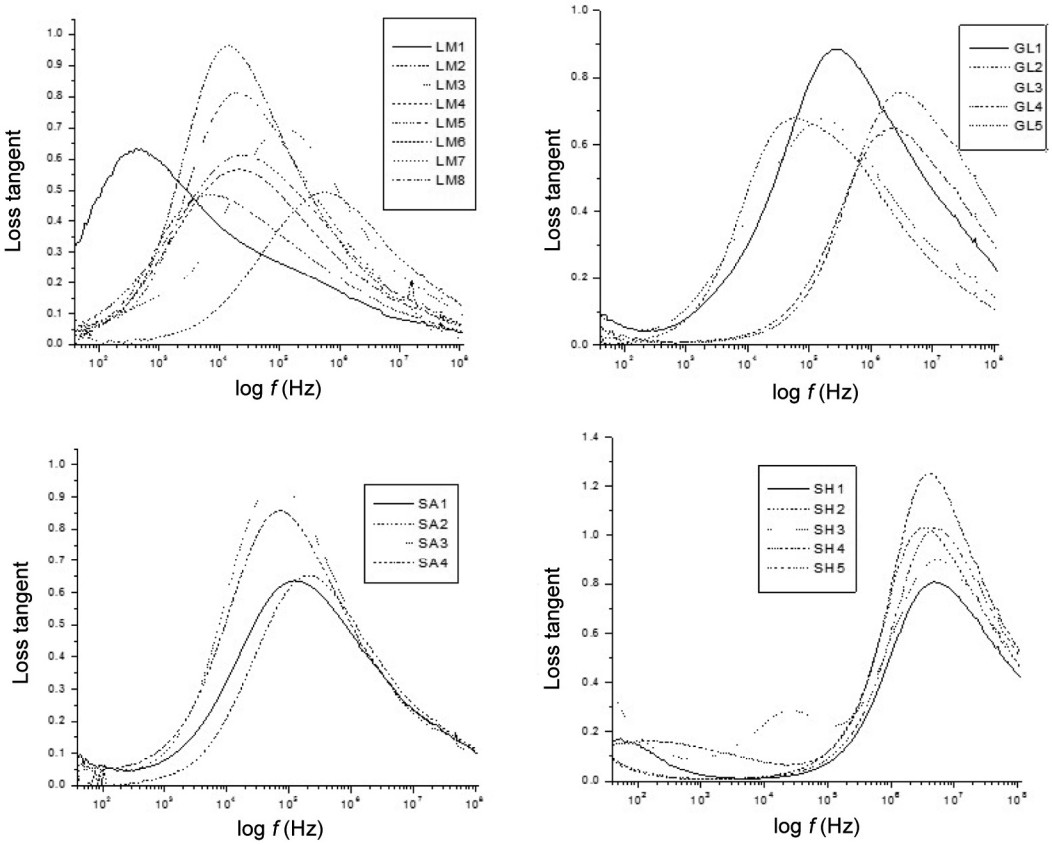

Figure 7. Plots of loss tangent against frequency for dry samples.

that are quite different. The ranges are shorter for limestone and sandstone than for shale and glauconite (Figure 3). Across the frequency range of measurement, the real relative permittivity of shale is the highest, followed by glauconite.

Limestone and sandstone exhibit low real relative permittivity values with respect to those of shale and glauconite. Clay/clay-like constituents in shale and glauconite result in charge build-up at grain boundaries which is partly responsible for their high ε_r' values[28,43]. Imaginary dielectric permittivity and loss tangent both show characteristic peaks at relaxation and critical frequencies respectively (Figures 5–8). Relaxation frequency, f_R, is generally high for shale (825 kHz–1.39 MHz), followed by glauconite (12.1–613 kHz). Limestone and sandstone have low values (1.75–57.2 kHz and 10.4–43.1 kHz respectively). The critical frequency, f_c, is higher than the corresponding relaxation frequency for all the samples: 3.13–4.89 MHz for shale; 89.2 kHz–2.70 MHz for glauconite; 61.6–202 kHz for sandstone and 21.8–569 kHz for limestone.

Figure 4 shows that for partially saturated rocks, the plateau region is extended while the dielectric dispersion region is shortened. This is due to: (i) the effect of electrode polarization which is usually more pronounced with rocks that are wet and conductive at low frequencies, and (ii) mobile ions in water adding to the conduction process. It is also observed that the dielectric constant values are higher for the saturated samples than for the dry ones, and is manifested in the broadening/stronger tail of the Cole–Cole plots (Figure 2). This is reflected in the upward shift in the frequency that separates the plateau and dispersion regions, which is 1.73–129 kHz for sandstone; 2.03–129 kHz for limestone, 103–139 kHz for glauconite, and 61.6–174 kHz for shale. The increase in ε_r' is related to interfacial polarization and electrochemical processes developed at the interfaces between rock mineral and electrolytic solutions[25,26]. Also, water itself has a high dielectric permittivity.

Greater ε_r' values in shale are due to higher concentration and distribution of thin, plate-like objects[44]. In addition to these effects, dielectric properties of rocks are also influenced by the surface and geometrical effects. Clay particles, being both highly surface-active and plate-like, will contribute further to the real relative permittivity by both mechanisms[44]. Also, interactions between charged clays and aqueous electrolytes give rise to an ionic double layer around those particles. Polarization of such a layer by an applied electric field has been identified as the main mechanism for the anomalous behaviour observed in rocks, soils and other biphasic systems of charged particles[45]. Gruner[46] reported that glauconite

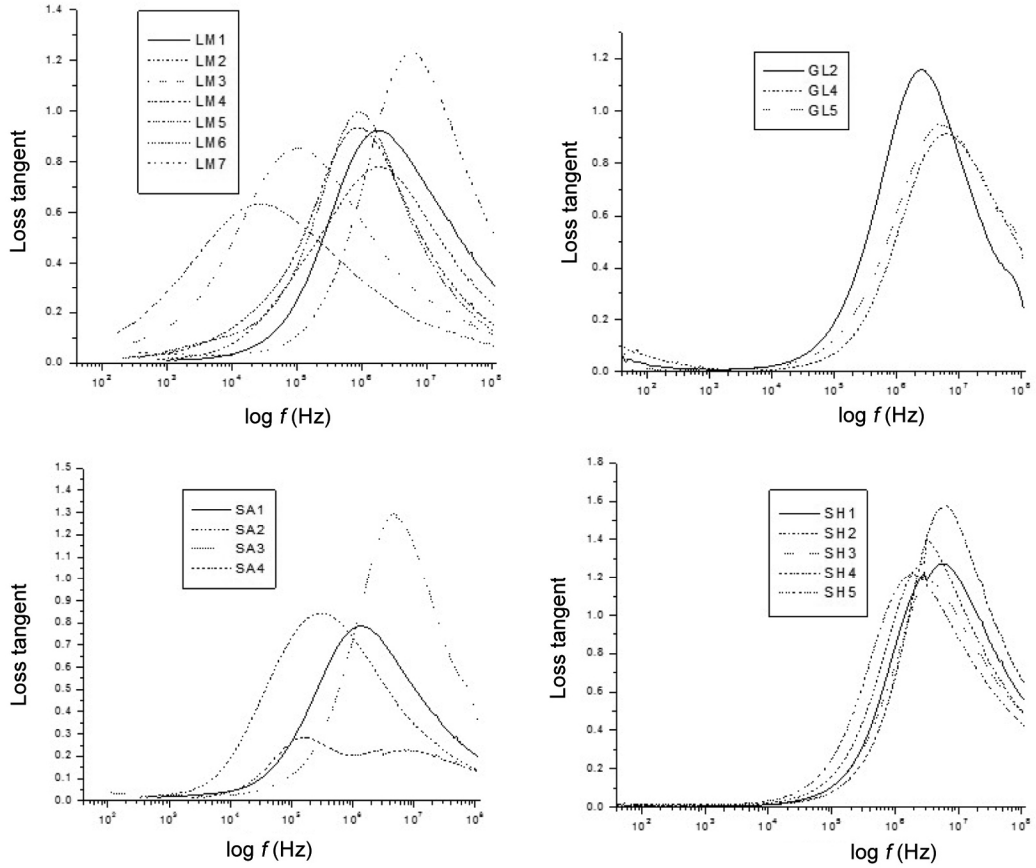

Figure 8. Plots of loss tangent against frequency for partially saturated samples.

is similar to the layer structures of mica, kaolinites vermiculite or chlorite (clay family). Jarrar *et al.*[47] described its structure as sheet-like, while Odin and Matter[48], as well as Odin[49] designated it as a dark green pelletal structure. Hence, due to its supposed clay mineral content and structure, the real relative permittivity of glauconite is a little less than that of shale. On the other hand, limestone and sandstone have grain-like and coarse structure, and as a result have lower real relative permittivity values relative to those of shale and glauconite.

Imaginary relative permittivity and loss tangent variations at partial saturation depict the characteristic bell-shaped curve (Figures 6 and 8 respectively) with relaxation and critical frequencies which are about an order greater than the respective frequencies for samples in dry condition. The dielectric enhancement is caused by the presence of electrolyte ions that are polarized around grains as the oscillating field is applied[21]. The Maxwell–Wagner effect occurs, where a discontinuity in conductivity between adjacent grains causes charge build-up leading to an additional capacitive impedance. Furthermore, it is well known that the low-frequency dielectric constant of a material made up of a layer of insulating material covered with a layer of conducting material can be extremely large when the concentration of the insulating region becomes small[44]. Also, it has been shown that in well-logging application, real dielectric permittivity (dielectric constant) is not sensitive to salinity at high frequencies[50]. The decrease in relaxation and critical frequencies at partial saturation for shale in contrast to the increase in these frequencies for the other three rock types points to the effect of pore geometry on overall dielectric relaxation.

Conclusion

The measured dielectric properties of the various rock types from Ewekoro quarry in Eastern Dahomey Basin have shown distinct variation in the entire frequency range on dry and saturated samples. This has established the usefulness of dielectric measurement as a diagnostic tool in rock raw material characterization. The complex plane plots (Cole–Cole plots) of all the rock samples indicate Cole–Cole relaxation type, which depicts a distribution of relaxation times. Each rock type is a multi-component system, which is in agreement with the result from geochemical analysis. All the rock types show dispersion in real and imaginary dielectric permittivity in dry and partially saturated conditions. However, the

frequency range for this dispersion differs for each rock type and is dependent on the level of saturation. Variations of real and imaginary dielectric permittivities and loss tangent are similar for both dry and partial water-saturated rocks, except in magnitude. In partial saturation there is: (i) enhanced polarization with consequent increase in all the electrical parameters of the rocks, and (ii) a shortening of the region of dielectric dispersion. Frequency-dependent characteristics of these rocks show that irrespective of their conditions (dry or saturated), the real relative permittivity of shale and glauconite is found to be significantly higher than that of limestone and sandstone. Similarly, the imaginary relative permittivity and loss tangent associated with shale and glauconite are of greater magnitude than for limestone and sandstone. Geometric or textural effects are partly responsible for these observed differences coupled with the presence of charged clay/clay-like particles in shale and glauconite. These observable differences in electrical properties/signatures can be utilized as a diagnostic tool for differentiation among these rocks to complement the traditional analysis such as geochemical analysis.

1. Cook, N. J., Mineral characterization of industrial mineral deposits at the Geological Survey of Norway: a short introduction. *NGU Bull.*, 2000, **436**, 189–192.
2. Worrell, E., Galitsky, C. and Price, L., Energy efficiency improvement opportunities for the cement industry. Environmental Energy Technologies Division LBNL-72E, Berkeley National Laboratory, CA, USA, 2008.
3. Harrison, D. J., Industrial mineral laboratory manual – limestone. Technical Report WG/92/29, Mineralogy and Petrology Series, British Geological Survey, UK, 1993.
4. British Geological Survey, UK, Mineral Profile-Cement Raw Materials, 2005, p. 20.
5. van Straaten, P., Rocks for crops: agrominerals for Sub-Saharan Africa. ICRAF, Nairobi, Kenya, 2002, pp. 227–230.
6. Kogbe, C. A., The Cretacious and Paleocene sediments of southern Nigeria. In *Geology of Nigeria* (ed. Kogbe, C. A.), Abiprint and Pak Ltd, Ibadan, Nigeria, 1975, p. 436.
7. Schneider, H., A study of glauconite. *J. Geol.*, 1927, **35**(4), 289–310.
8. Aldieb, M. A. and Ibrahim, H. G., Variation of feed chemical composition and its effect on clinker formation–simulation process. In Proceedings of the World Congress on Engineering and Computer Science, San Francisco, USA, 20–22 October 2010, vol. 2.
9. Josh, M., Clennell, B. and Siggins, A. Practical broadband dielectric measurement of geological materials. In SPWLA 50th Annual Logging Symposium, Texas, USA, 21–24 June 2009.
10. Josh, M., Esteban, L., Delle Piane, C., Sarout, J., Dewhurst, D. N. and Clennell, M. B., Laboratory characterization of shale properties. *J. Petr. Sci. Eng.*, 2012, **88**, 107–124.
11. Knight, R. J., The dielectric constant of sandstones: 5 Hz to 13 MHz: Ph D thesis, Stanford University, USA, 1984.
12. Knight, R., The use of complex plane plots in studying the electrical response of rocks. *J. Geomagn. Geoelectr.*, 1984, **35**, 767–776.
13. Knight, R. J. and Nur, A., The dielectric constant of sandstones, 50 kHz to 4 MHz. *Geophysics*, 1987, **52**, 644–654.
14. Knight, R. J. and Nur, A., Geometrical effects in the dielectrical response of partially saturated sandstones. *Log Anal.*, 1987, **28**, 513–519.
15. Garrouch, A. A. and Sharma, M. M., Dielectric dispersion of partially saturated porous media in the frequency range 10 Hz to 10 MHz. *Log Anal.*, 1998, **39**, 48–53.
16. Garrouch, A. A., A systematic study revealing resistivity dispersion in porous media. *Log Anal.*, 1999, **40**, 271–279.
17. Adisoemarta, P. S., Complex electrical properties of shale as a function of frequency and water content. Ph D thesis, Texas Tech University, Texas, USA, 1999.
18. Seleznev, N. V., Theoretical and laboratory investigation of dielectric properties of partially saturated carbonate rocks. Ph D thesis, TU Delft, The Netherlands, 2005.
19. Josh, M., Dielectric permittivity: a petrophysical parameter for shales. *Petrophysics*, 2014, **55**(4), 319–332.
20. Knight, R. J. and Endres, A. L., A new concept in modeling the dielectrical response of sandstones: defining a wetted rock and bulk water system. *Geophysics*, 1990, **55**, 586–594.
21. Garrouch, A. A. and Sharma, M. M., The influence of clay content, salinity, sress, and wettability on the dielectric properties of brine-saturated rocks: 10 Hz to 10 MHz. *Geophysics*, 1994, **59**(6), 909–917.
22. Gomaa, M. M., Relation between electric properties and water saturation for hematitic sandstone with frequency. *Ann. Geophys.*, 2008, **51**(5/6), 801–811.
23. Toumelin, E., Torres-Verdin, C. and Bona, N., Improving the petrophysical assessment of rock-fluid systems with wide-band electromagnetic measurements. In Annual Technical Conference and Exhibition, Dallas, Texas, USA, SPE 96258, 9–12 October 2005.
24. Toumelin, E., Torres-Verdin, C. and Bona, N., Improving petrophysical interpretation with wide-band electromagnetic measurements. *SPE J.*, 2008, **13**(2), 205–215.
25. Chelidze, T. L. and Gueguen, Y., Electrical spectroscopy of porous rocks: a review – I. Theoretical models. *Geophys. J. Int.*, 1999, **137**, 1–15.
26. Chelidze, T. L., Gueguen, Y. and Ruffet, C., Electrical spectroscopy of porous rocks: a review – II. Experimental results and interpretation. *Geophys. J. Int.*, 1999, **137**, 16–34.
27. Bigakle, J., A study concerning the conductivity of porous rock. *Phys. Chem. Earth*, 2000, **A25**, 189–194.
28. Sengwa, R. J. and Soni, A., Dielectric properties of some minerals of western Rajasthan. *Indian J. Radio Space Phys.*, 2008, **37**, 57–63.
29. Knight, R. J. and Abad, A., Rock/water interaction in dielectric properties: experiments with hydrophobic sandstones. *Geophys.*, 1995, **60**(2), 431–436.
30. Fechner, T., Börner, F. D., Richter, T., Yaramanci, U. and Weihnacht, B., Lithological interpretation of the spectral properties of limestone. *Near Surf. Geophys.*, 2004, **3**, 150–159.
31. Bekhit, M. M. and Khalil, S. A., Electrical properties of moist limestone samples in the frequency range 1 Hz–10 MHz from Abu Rawash Area. *Aust. J. Basic Appl. Sci.*, 2007, **1**(4), 741–750.
32. Hu, K. and Liu, C. R., Theoretical study of the dielectric constant in porous sandstone saturated with hydrocarbon and water. *IEEE Trans. Geosci. Remote Sensing*, 2000, **38**(3), 1328–1336.
33. Szerbiak, R. B., McMechan, G. A. Forster, C. and Snelgrove, S. H., Electrical and petrophysical modelling of Ferron sandstone. *Geophysics*, 2006, **71**, 197–210.
34. Fam, M. A. and Dusseault, M. B., High-frequency complex permittivity of shales (0.02–1.30 GHz). *Can. Geotech. J.*, 1998, **35**(3), 524–531.
35. Sweeney, J., Roberts, J. and Harben, P., Study of dielectric properties of dry and saturated Green River oil shale. *Energy Fuels*, 2007, **21**, 2769–2777.
36. Środoń, J., Drits, V. A., MCcarty, D. K., Hsieh, J. C. C. and Eberl, D. D., Quantitative X-ray diffraction analysis of clay-bearing rocks from random preparation. *Clays Clay Miner.*, 2001, **49**(6), 514–528.

37. Obiajunwa, E. I. and Nwachukwu, J. I., Elemental analysis of limestone samples from Ewekoro limestone deposit in southwest Nigeria. *Nucl. Instrum. Meth. Phys. Res. B*, 2000, **170**, 427–431.
38. Cole, K. S. and Cole, R. H., Dispersion and absorption in dielectrics. *J. Chem. Phys.*, 1941, **9**, 341–351.
39. Debye, P., *Ver. Deut. Phys. Gesell.*, 1913, **15**, 777; reprinted in collected papers of Peter J. W. Debye, Interscience, New York, 1954.
40. Debye, P., *Polar Molecules*, Dover Publication, New York, USA, 1929.
41. Jonsher, A. K., Dielectric relaxation in solids. *J. Phys. D: Appl. Phys.*, 1999, **32**, R57–R70.
42. Olhoeft, G. R., Electrical properties of rocks. In *Physical Properties of Rocks and Minerals* (eds Touloukian, Y. S., Judd, W. R. and Roy, R. F.), McGraw-Hill, New York, 1976.
43. Sen, P. N., Relation of certain geometric features to the dielectric anomaly of rocks. *Geophysics*, 1981, **46**, 1714–1720.
44. Sen, P. N. and Chew, W. C., The frequency dependent dielectric and conductivity response of sedimentary rocks. *J. Microwave Power*, 1983, **18**(1), 95–105.
45. Chew, W. C. and Sen, P. N., Dielectric enhancement due to electrochemical double layer: thin double layer approximation. *J. Chem. Phys.*, 1982, **77**(9), 4683–4693.
46. Gruner, J. W., The structural relationship of glauconite and mica. *J. Mineral. Soc. Am.*, 1935, **20**, 699–714.
47. Jarrar, G., Amireh, B. and Zachmann, D., The major, trace and rare earth element geochemistry of glauconites from the early Cretaceous Kurnub Group of Jordan. *Geochem. J.*, 2000, **34**, 207–222.
48. Odin, G. S. and Matter, A., De glauconiarum origine. *Sedimentology*, 1981, **28**, 611–641.
49. Odin, G. S., Green marine clays. In *Development in Sedimentology*, Amsterdam, Elsevier, 1988, p. 45.
50. Myers, M. T., A saturation interpretation model for the dielectric constant of shaly sands. SCA Conference Paper 9118, San Antonio, Texas, USA, August 1991.

ACKNOWLEDGEMENTS. We thank Commonwealth Scientific and Industrial Organization (CSIRO), Earth Science and Resource Engineering, Perth, Western Australia for providing the necessary facilities (Agilent 4294A, test kit and probe, humidity chamber); Mike Verrall useful discussions and technical assistance, and Emma Crooke for assistance during the visit of the O.O.B. to CSIRO.

Received 22 April 2016; revised accepted 2 January 2017

doi: 10.18520/cs/v113/i02/253-263